JOURNAL OF MATERIALS SCIENCE 31 (1996) 2893–2896

Influence of Ar ion etching on T_c of liquid-quenched $Bi_{1.6}Pb_{0.4}Sr_2Ca_2Cu_3O_x$ superconductor by sheet plasma source

YOSHITAKE NISHI, HIROKAZU ISHII, KAGEYOSHI SAKAMOTO, KAZUYA OGURI, HISAKUNI MATSUMOTO*, AKIRA TONEGAWA*, KAZUO TAKAYAMA**

*Department of Materials Science, and * Department of Physics, and ** Institute of Research & Development, Tokai University, 1117 Kitakaname, Hiratsuka Kanagawa, 259-12, Japan*

The influence of argon-ion etching is investigated for liquid-quenched high-T_c $Bi_{1.6}Pb_{0.4}Sr_2Ca_2Cu_3O_x$. The argon-ion irradiation has no effect on the T_c value for a dose of 4.05×10^{17} (ions mm^{-2}). However, doses in excess of this level greatly decreases the T_c value. Therefore, a critical irradiation does value (D_c) to maintain a T_c value above 100 K is defined and determined. The D_c is about 4.94×10^{17} (ions mm^{-2}) for argon-ion irradiation at the low acceleration energy of 1 keV.

1. Introduction

The ion etching technique is known to be a good process for etching brittle materials [1–3]. The application of this technique to the cuprate high temperature superconductors is limited by the observation that an excessive amount of irradiation decreased the superconducting transition temperature, T_c, to below 4.2 K [4].

Since one of the potential applications of the oxide high T_c superconductors is in superconducting magnets for fusion reactors it is of interest to obtain information on the effect of radiation damage on the superconducting properties of these materials.

The production of $Bi_{1.6}Pb_{0.4}Sr_2Ca_2Cu_3O_x$ superconducting samples by the annealing of glassy foils produced by liquid quenching offers a quicker route to denser samples than those obtained by conventional sintering techniques.

In this paper, the influence of argon-ion irradiation on T_c is investigated for a high-T_c $Bi_{1.6}Pb_{0.4}Sr_2Ca_2Cu_3O_x$ sample which was produced by the crystallization of a liquid quenched glassy foil. The critical irradiation dose value (D_c) to maintain a T_c value above 100 K has been determined.

2. Experimental procedure

Samples with nominal composition $Bi_{1.6}Pb_{0.4}Sr_2Ca_2Cu_3O_x$ were prepared from high-purity powders of Bi_2O_3 (99.99%), PbO (99.99%), $SrCO_3$ (99.99%), $CaCO_3$ (99.99%), and CuO (99.9%). The powders were mixed and reacted in air at 1023 K for 6 h and then air cooled. After crushing, the sintered powders were resintered in air at 1073 K for 18 h and then air cooled. After crushing, pellets, 0.8 mm thick and 13 mm in diameter, were resintered in air at 1123 K for 12 h and then furnace cooled. This sintered sample was used to make the liquid quenched glassy foils.

The foils were prepared from chips cut from the sintered pellet using a twin-type piston–anvil apparatus [6]. This apparatus was constructed to quench the molten sample in a quartz tube. The amount of sample melted by an infrared furnace in a single experiment was about 0.2 g. The speed of the piston was about 0.12 m s^{-1}. The cooling rate was varied by controlling the sample mass [7]. The sample for ion irradiation was of about 95 μm thickness, and was crystallized at 1123 K for 40 h and furnace cooled.

The electrical resistivity was measured by the standard four-probe technique using a Keithley 181 nanovoltmeter. The probes were attached onto the etched sample surface. The temperature was measured by a Au Fe-chromel thermocouple attached to the sample which was contained in a calibrated cryostat. Fig. 1 shows the measured temperature dependence of the resistivity of the $Bi_{1.6}Pb_{0.4}Sr_2Ca_2Cu_3O_x$ sample. The temperature of zero resistivity, T_c^0 was taken to be the point at which the measured resistivity was below 10^{-9} Ωm at a measuring current density of 0.2 mA mm^{-2}. The onset point of the superconductivity is taken at $d(R/R^{300K})/dT = 0.004$, where $d(R/R^{300K})/dT$ and R^{300K} are the slope of the resistivity versus temperature graph and the resistivity at 300 K, respectively. The onset temperature is designated as T_c^{on}.

The structure of the sample was monitored by X-ray-diffraction (model RU-200B, Rigaku Denki, Tokyo). The diffraction was performed using a step scanning method (Cu target, 40 kV, 50 mA, 0.01 deg/step, 20 s/step).

The ion beam irradiation was performed under a 3×10^{-5} Torr argon atmosphere using a sheet plasma source [9]. Fig. 2 is a schematic representation of the experimental configuration. A sheet plasma was created by compressing the generated plasma with a magnetic field, into a sheet shape whose thickness was

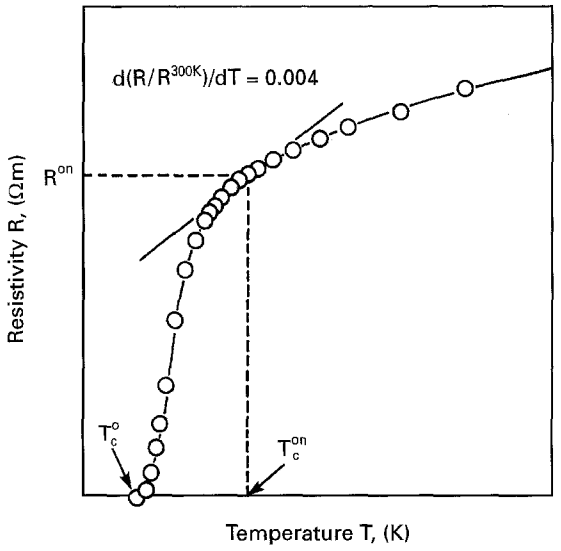

Figure 1 Change in electrical resistivity (R) against temperature (T) for $Bi_{1.6}Pb_{0.4}Sr_2Ca_2Cu_3O_x$.

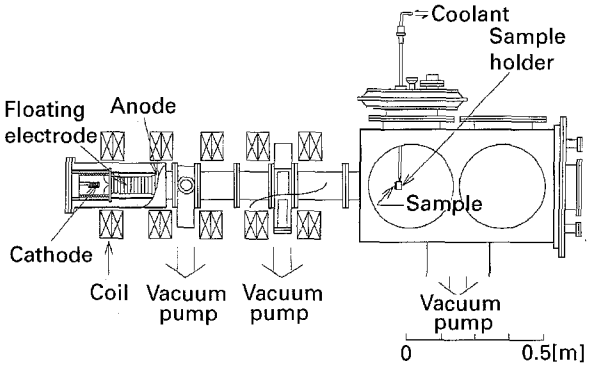

Figure 2 Schematic drawing of sheet plasma source.

the same as the average ion cyclotron diameter. Since its density, temperature and plasma potential distributions all showed a wide horizontal plateau, the sheet plasma could be applied for horizontally homogeneous irradiation. The energy for ion acceleration was 1.0 keV and the ion irradiation current density was about 2.2 mA cm^{-2}. These values being obtained by measurements using a Digital voltmeter and a Faraday-cup, respectively. The total irradiation dose was calculated using the following formula.

$$\text{Dose (ions mm}^{-2}) = (Dt_i/e) \qquad (1)$$

where D, t_i and e are the irradiation current density (A mm^{-2}), the irradiation time(s) and the electron charge (1.602×10^{-9} C), respectively. The ion beam was perpendicular to the sample surface. The sample holder was held at room temperature during the irradiation by water cooling and the sample temperature controlled by this cooling was monitored by means of a chromel–alumel thermocouple attached to the unirradiated side of the sample.

3. Results and discussion

3.1. Changes in the lattice constant through Ar ion irradiation

The XRD technique was used to investigate any structural changes associated with the irradiation. Fig. 3

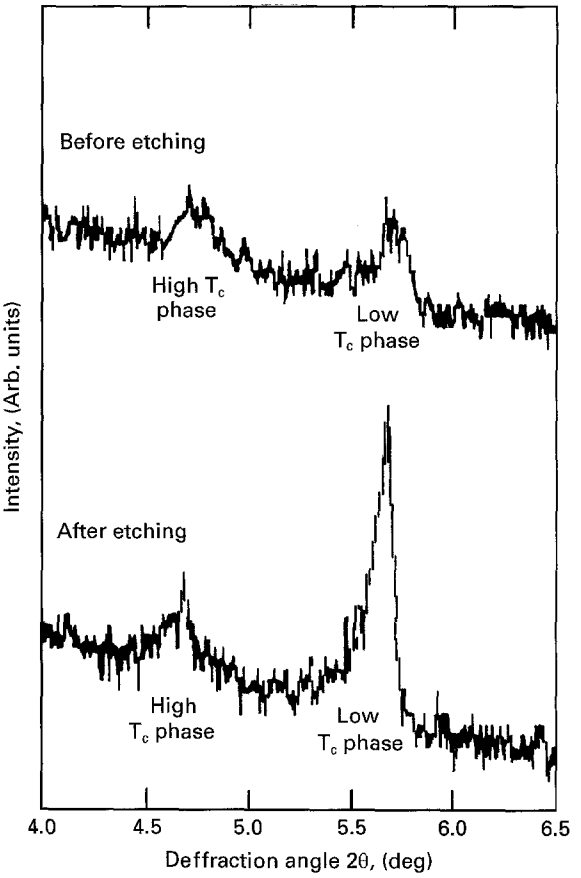

Figure 3 X-ray-diffraction patterns of (002) reflections of $Bi_{1.6}Pb_{0.4}Sr_2Ca_2Cu_3O_x$ before and after argon-ion etching (Dose = 5.82×10^{17} ions mm^{-2} at 0° ion-beam angle).

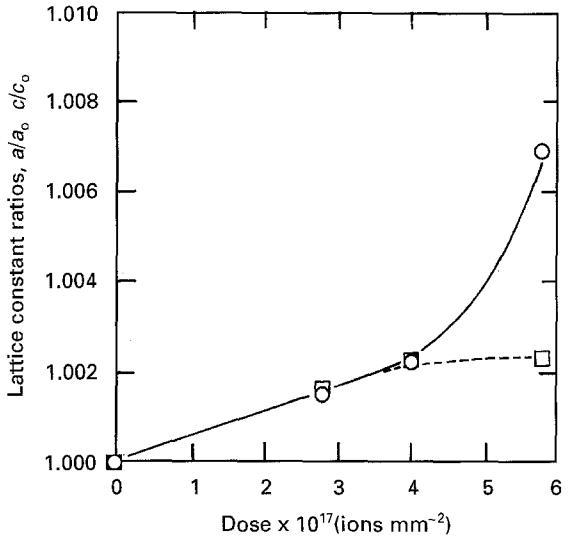

Figure 4 Changes in lattice constant ratios of high-T_c phase against argon-ion irradiation dose for $Bi_{1.6}Pb_{0.4}Sr_2Ca_2Cu_3O_x$. The c/c_0 ratio is represented by the symbol (○) and the a/a_0 ratio is represented by the symbol (□).

shows the (002) reflection of the high and low T_c phases in $Bi_{1.6}Pb_{0.4}Sr_2Ca_2Cu_3O_x$ before and after irradiation. The peaks of both the high-T_c and low-T_c phases shift to a lower 2θ angle with excess irradiation. In addition the relative intensities of the two peaks change with the (002) reflection of the low-T_c phase becoming dominant.

Fig. 4 shows the changes in the lattice constants for the high-T_c phase with the irradiation dose for

$Bi_{1.6}Pb_{0.4}Sr_2Ca_2Cu_3O_x$ with a_0, c_0 and a, c being the lattice constants before and after the irradiation respectively. The a/a_0 and c/c_0 values are observed to increase with the c/c_0 ratio increasing to a greater extent than a/a_0 which saturates at high irradiation doses. Fig. 3 suggests that argon atoms are implanted into the structure and thus elongate the c lattice constant.

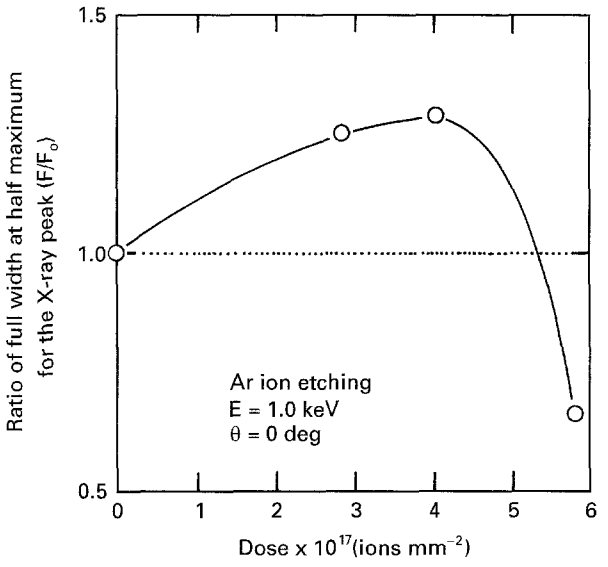

Figure 5 Changes in reduced width of X-ray-diffraction peaks at half height of high-T_c phase against argon-ion irradiation dose for $Bi_{1.6}Pb_{0.4}Sr_2Ca_2Cu_3O_x$.

Fig. 5 shows the change in the full width at half maximum (FWHM) of the X-ray-diffraction peaks in the high-T_c phase against the irradiation dose. Here, F_0 and F are the FWHM of the peaks before and after the irradiation, respectively. Fig. 5 shows that F/F_0 increases with higher irradiation doses up to about 4×10^{17} (ions mm^{-2}) and that beyond this dose it begins to fall reaching lower values than those observed before the etching. The F/F_0 ratio can be interpreted as indicating the degree of crystalline perfection. Thus the results of this experiment can be understood as that a low implantation dose randomizes the crystal lattice order but that a larger dose expands the lattice and certain stress-relaxation processes occurred in order to improve the lattice order.

Based on the above results, an implantation model has been devised (see Fig. 6). In this model, the irradiation homogeneously implants argon ions into the crystal lattice which randomize the lattice. At irradiation doses above 4×10^{17} (ions mm^{-2}) the F/F_0 value decreases tremendously, whereas the c/c_0 value rapidly increases. The decrease in F/F_0 probably reflects the relaxation of the residual stress in the sample introduced by the implanted argon ions. If there is a relaxation stage, then microcracking and twinning may occur which would cause T_c to decay. Thus, it is important to examine the influence of the irradiation on the superconducting properties of the sample.

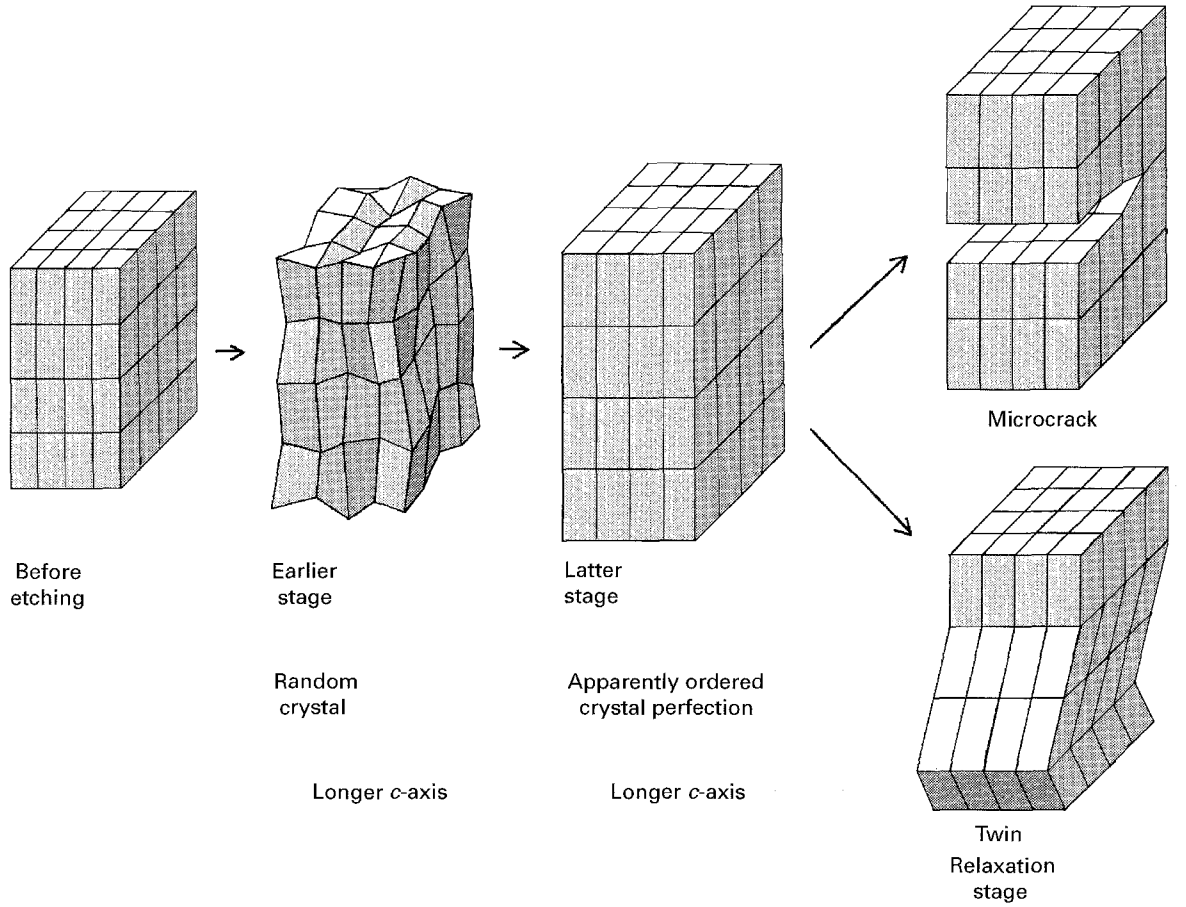

Figure 6 Model for argon ion implantation.

3.2. T_c decay

Fig. 7 shows the changes in the onset and full entry into the superconducting state temperatures (T_c^{on} and T_c^0) against the argon-ion irradiation dose for the $Bi_{1.6}Pb_{0.4}Sr_2Ca_2Cu_3O_x$. The irradiation has no effect on T_c for doses of 4.05×10^{17} (ions mm^{-2}), but beyond this level it greatly decreases the T_c^{on} and T_c^0 values to the point that at a dose of 5.82×10^{17} (ions mm^{-2}) no T_c value is observed above 4.2 K. Thus we have determined the critical irradiation dose ($D_c = 4.94 \times 10^{17}$ ions mm^{-2}) that maintains a T_c value above 100 K for a liquid-quenched and crystallized $Bi_{1.6}Pb_{0.4}Sr_2Ca_2Cu_3O_x$ sample.

3.2. Electrical resistivity

The carrier concentration (c^*) is one of the dominant factors that control the T_c and thus, the electrical resistivity should contribute to the T_c change. Fig. 8 shows the changes in the electrical resistivity ratio R/R_0 against the argon-ion irradiation dose at 150 and 300 K. Here, R_0 and R are the measured electrical resistivities before and after the argon-ion irradiation, respectively. At argon-ion irradiation doses below 4.05×10^{17} (ions mm^{-2}) the R/R_0 ratio does not change much. However above this threshold the R/R_0 ratio is observed to greatly increase. This increase in resistivity results in a smaller density of state, and hence to a smaller c^* which is reflected in the T_c decay observed in Fig. 2.

The decay in T_c is considered to be due to the argon ions becoming implanted in the sample and creating microcracks and twinning which act so as to decrease the carrier concentration, here decreasing the T_c value. This concept is schematically represented in Fig. 4.

We also measured the properties of the unirradiation side of the samples and again observed the decay in T_c with high irradiation doses. This suggests that almost the whole volume of the sample is affected by the irradiation.

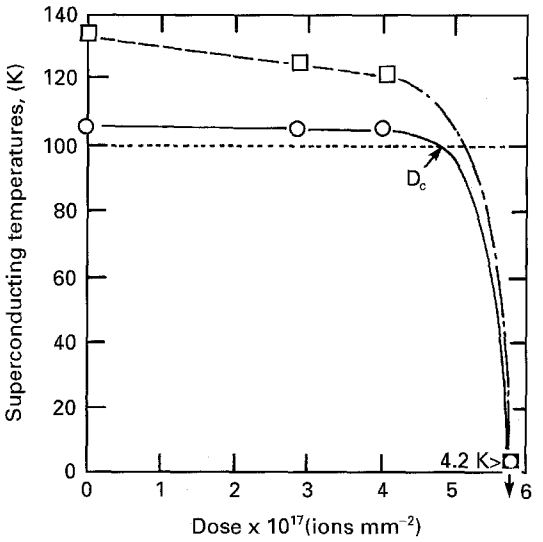

Figure 7 Changes in onset and full superconducting temperatures (T_c^{on} and T_c^0) against argon-ion irradiation dose for $Bi_{1.6}Pb_{0.4}Sr_2Ca_2Cu_3O_x$. The T_c^{on} values are represented by the (□) symbol and the T_c^0 values by the (○) symbol.

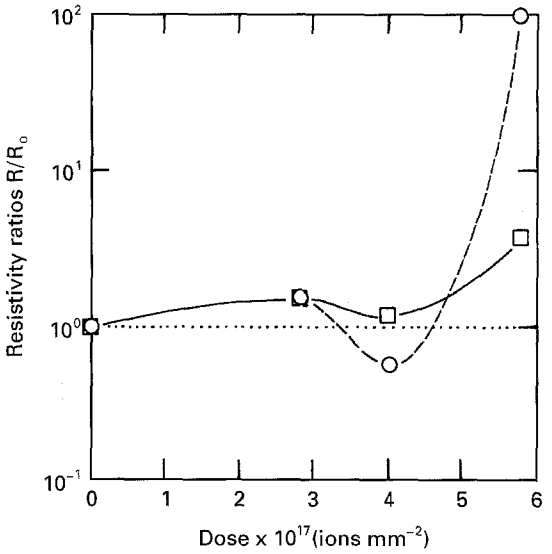

Figure 8 Changes in the electrical resistivity ratio R/R_0 at 150 K and 300 K against argon-ion irradiation dose for $Bi_{1.6}Pb_{0.4}Sr_2Ca_2Cu_3O_x$. Where the data taken at 150 K is represented by the symbol (○) and the data taken at 300 K by the symbol (□).

4. Conclusion

In summary, high argon-ion irradiation doses decay the T_c^0 values to below 4.2 K. The critical irradiation dose D_c to maintain a T_c value above 100 K is about 4.94×10^{17} (ions mm^{-2}).

References

1. N. INOUE, Y. TAKAHASHI, T. SUDO, K. SAKAMOTO, T. SHIMA and Y. NISHI, *J. Appl. Phys.* **71** (1992) 347.
2. A. F. HEBARD, R. M. FLEMING, K. T. SHORT, A. E. WHITE, C. E. RICE, A. F.J. LEVI and R. H. ELICK, *Appl. Phys. Lett.* **55** (1989) 1915.
3. Y. NISHI, S. MORIYA, N. INOUE, S. TOKUNAGA and T. SHIMA, *J. Mater. Sci. Lett.* **7** (1988) 281.
4. *Idem, ibid.* **7** (1988) 997.
5. Y. NISHI, S. MORIYA and T. MANABE, *J. Appl. Phys.* **65** (1989) 2389.
6. Y. NISHI, M. TACHI and M. TAKIGAWA, *Wear* **110** (1986) 83.
7. Y. NISHI, K. SUZUKI and T. MASUMOTO, *J. Jpn Inst. Metals.* **45** (1981) 1300.
8. Y. NISHI, K. OGURI, H. OHINATA, K. TANIOKA, Y. KITA and N. NINOMIYA, *Phys. Rev. B* **41** (1990) 6520.
9. K. SUNAKO, K. YAMAUCHI, T. NOGUCHI, T. NIHEI, H. WATANABE, T. TANIKAWA, K. TAKAYAMA and T. TSUGUEDA, *Nucl. Instr. and Meth. B* **37** (1989) 636.
10. N. M. TALLAN and I. BRANSKY, *J. Electrochem. Soc.* **118** (1971) 345.
11. R. F. BREBRICK, in "Defects in Solids, Vol. 2 of Treatise on Solid State Chemistry", edited by N. B. Hannay (Plenum, New York, 1975) pp. 357–362.
12. Y. NISHI, K. NOZAKI and K. TAKUYA, *Z. Phys. B* **91** (1993) 175.

Received 25 April 1995
and accepted 1 December 1995